



# HHS Public Access

Author manuscript

*Cell Cycle*. Author manuscript; available in PMC 2016 August 02.

Published in final edited form as:

*Cell Cycle*. 2009 December 15; 8(24): 4112–4118. doi:10.4161/cc.8.24.10215.

## Pseudo-DNA damage response in senescent cells

Tatyana V. Pospelova<sup>1,\*</sup>, Zoya N. Demidenko<sup>2</sup>, Elena I. Bukreeva<sup>1</sup>, Valery A. Pospelov<sup>1</sup>,  
Andrei V. Gudkov<sup>3</sup>, and Mikhail V. Blagosklonny<sup>2,3,\*</sup>

<sup>1</sup>Institute of Cytology; Russian Academy of Sciences; St. Petersburg, Russia

<sup>2</sup>Oncotarget; Buffalo, NY USA

<sup>3</sup>Department of Cell Stress Biology; Roswell Park Cancer Institute; BLSC; Buffalo, NY USA

### Abstract

Cellular senescence is currently viewed as a response to DNA damage. In this report, we showed that non-damaging agents such as sodium butyrate-induced p21 and ectopic expression of either p21 or p16 cause cellular senescence without detectable DNA breaks. Nevertheless, senescent cells displayed components of DNA damage response (DDR) such as  $\gamma$ H2AX foci and uniform nuclear staining for p-ATM. Importantly, there was no accumulation of 53BP1 in  $\gamma$ H2AX foci of senescent cells. Consistently, comet assay failed to detect DNA damage. Rapamycin, an inhibitor of mTOR, which was shown to suppress cellular senescence, decreased  $\gamma$ H2AX foci formation. Thus, cellular senescence leads to activation of atypical DDR without detectable DNA damage. Pseudo-DDR may be a marker of general over-activation of senescent cells.

### Keywords

DNA damage; DDR; cellular senescence; aging;  $\gamma$ H2AX; p21; cell cycle

### Introduction

DNA damage can cause apoptosis, reversible cell cycle arrest and cellular senescence, characterized by irreversible loss of proliferative potential. DNA damage results in phosphorylation of ATM, which in turn phosphorylates  $\gamma$ H2AX as an initial part of DNA damage response (DDR). Phosphorylated  $\gamma$ H2AX, known as  $\gamma$ H2AX, functions to hold broken chromosome ends and to recruit DNA repair proteins nearby of DNA damage.<sup>1-3</sup>  $\gamma$ H2AX-foci also contain p-ATM and 53BP1 (p53-binding protein 1). DDR can lead to cell cycle arrest. In turn, prolonged cell cycle arrest culminates in cellular senescence, if the mTOR pathway is over-activated.<sup>4,5</sup> Therefore, senescence is characterized by cellular hyper-activation, including hyper-secretory and pro-inflammatory phenotypes, excessive mass growth (a large cell morphology), increased levels of cyclin D1, inappropriate S-phase re-entry associated with the loss of proliferative potential.<sup>6-8</sup> Cellular over-activation could be linked to organismal aging.<sup>8,9</sup> Importantly, inhibitors of the PI-3K/mTOR pathway

\*Correspondence to: Tatyana V. Pospelova and Mikhail V. Blagosklonny; tvpgroup@mail.ru and Blagosklonny@oncotarget.com. Supplementary materials can be found at: [www.landesbioscience.com/supplement/PospelovaCC8-24-Sup.pdf](http://www.landesbioscience.com/supplement/PospelovaCC8-24-Sup.pdf)

partially suppress cellular senescence.<sup>5,10,11</sup> Like PI-3K and mTOR, the ATM kinase belongs to the PI-3K family of kinases.<sup>12</sup> By analogy with activation of the PI-3K/mTOR pathway, senescence might be associated with activation of related signaling pathways. If so, then DDR may be present in senescent cells, even in the absence of DNA damage. To address this hypothesis, we measured DDR following the induction of senescence by non-damaging inducers such as the HDAC inhibitor sodium butyrate, overexpression of cyclin-dependent kinase inhibitors p21 and p16. In human HT1080 and rodent E1A + Ras-transformed cells, these factors cause cellular senescence characterized by cellular hypertrophy, beta-Gal-staining and permanent loss of proliferative capacity, partially preventable by rapamycin.<sup>5</sup> Here we investigated whether senescent cells exhibit DDR as a marker of inappropriate over-activation of growth and stress signaling pathways.

## Results

### DDR in sodium butyrate-induced senescence

As we described recently, sodium butyrate (NaB), a HDAC inhibitor, induced p21-dependent cellular senescence in E1A + Ras-transformed rodent cells.<sup>13</sup> NaB-induced cellular senescence was characterized by G<sub>1</sub> arrest, permanent loss of proliferative potential (cells did not resume proliferation, even when NaB was removed), a large and flat morphology and beta-Gal-staining.<sup>5,13</sup> Here we show that DNA damage response (DDR) became prominent by day 5 (**Fig. 1**). First,  $\gamma$ H2AX foci became detectable, with increasing intensity from days 1 to 5. Treatment with NaB increased  $\gamma$ H2AX foci nearly four-fold after one day of treatment, while a trace of p-ATM was detectable in the nucleus, but not in the foci at that time. Second, p-ATM became detectable in the nucleus later and p-ATM granular staining and  $\gamma$ H2AX foci were poorly colocalized (**Fig. 1**, lower). As shown in **Figure 1**,  $\gamma$ H2AX foci (red) predominated over mixed (yellow) foci and some p-ATM (green) was localized outside of the foci. In contrast, radiation-induced  $\gamma$ H2AX foci contained p-ATM (yellow). Most importantly, we could not detect 53BP1 (**Fig. 2**). In contrast, radiation-induced  $\gamma$ H2AX foci contained 53BP1 (**Fig. 2**). Thus, there was no accumulation of 53BP1 neither in fully senescent cells nor during senescence induction (**Fig. 3**). We conclude that  $\gamma$ H2AX is the most prominent marker of NaB-induced senescence and that  $\gamma$ H2AX foci are devoid of 53BP1. In contrast, radiation caused accumulation of  $\gamma$ H2AX, p-ATM and 53BP1 (**Fig. 1 and Suppl. Fig. 1**).

### Rapamycin decreased $\gamma$ H2AX foci in NaB-induced senescence

We have recently demonstrated that rapamycin suppressed NaB-induced senescence.<sup>5</sup> Next, we evaluated the effect of rapamycin on the senescent-associated DDR (**Fig. 4**). In senescent cells, the number of  $\gamma$ H2AX foci was elevated more than eight times (**Fig. 4**, NaB). Thus, levels of  $\gamma$ H2AX foci in senescent cells were approximately equal to levels of radiation-induced  $\gamma$ H2AX foci (**Fig. 4**). Rapamycin significantly blunted the amount of  $\gamma$ H2AX foci in NaB-treated senescent cells. Given that rapamycin suppresses cellular senescence,<sup>5</sup> this further suggests that  $\gamma$ H2AX foci are markers of senescent phenotype.

### No DNA breaks in NaB-induced senescence

Most importantly, there were no detectable DNA breaks in senescent cells as measured by the comet assay (**Fig. 5**), which detects DNA damage directly. Furthermore, there were no comets after brief (30 min) or long-term (2 and 5 days) treatments with NaB neither alone nor with rapamycin. Rapamycin alone also did not induce DNA breaks (**Fig. 5**), even though there was a marginal increase in  $\gamma$ H2AX foci (**Fig. 4**). In contrast, irradiation caused dramatic DNA breaks in all cells (**Fig. 5**). In spite of the difference in the induction of DNA breaks, irradiation and NaB caused comparable accumulation of  $\gamma$ H2AX foci (**Fig. 4**). Although the sensitivity of the comet assay is limited, it is the most sensitive direct method available. Even if NaB induced undetectable DNA damage (below the sensitivity of the most sensitive direct method comet assay), the accumulation of  $\gamma$ H2AX foci was not proportional to the damage.

### H2AX accumulation in p21- and p16-induced senescence

We extended our observation to well-studied models of IPTG-inducible p21- and p16-senescence in HT1080 cells, HT-p21a and HT-p16 clones.<sup>14,15</sup> Following induction of either p21 or p16 by IPTG, HT-p21a and HT-p16 cells undergo rapid G<sub>1</sub>/G<sub>2</sub> and G<sub>1</sub> arrest.<sup>4,5,14,15</sup> By day three, cells became senescent, characterized by a large flat morphology, beta-Gal-staining and permanent loss of proliferative potential.<sup>4,5,14,15</sup> Using flow cytometry, here we investigated whether there was an accumulation of  $\gamma$ H2AX in such senescent cells. After 3 days of IPTG treatment, levels of  $\gamma$ H2AX were increased in both HT-p21a cells and HT-p16 cells (**Fig. 6**). Noteworthy, IPTG did not induce  $\gamma$ H2AX at first day of the treatment, although these cells are already arrested at that time.<sup>4,5,14,15</sup> These results were confirmed by detection of  $\gamma$ H2AX foci by immunocytochemistry (**Suppl. Fig. 2**). Interestingly, IPTG-induced senescence did not lead to any changes of p53 levels.<sup>16</sup>

### Lack of DNA damage in p21-induced senescence

We next determined whether DNA damage could be detected by comet assay (**Fig. 7**). There were no comets in IPTG-treated senescent HT-p21a and HT-p16 cells (**Fig. 7**). As a positive control, we treated cells with doxorubicin to cause double strand breaks (neutral electrophoresis) and topotecan to cause single strand breaks (alkaline electrophoresis) (**Fig. 7**). Although it is impossible to exclude undetectable (below the sensitivity limit) DNA damage, we can exclude such undetectable damage as a cause of senescence. First, very low concentrations of peroxide (8 microM) induced DNA damage, easily detectable by the comet assay, but failed to cause cellular senescence at such low concentrations (data not shown). This indicates that HT-p21a cells are resistant to cell cycle arrest caused by DNA damage. Second, p21- and p16-induced arrest preceded DDR, not vice versa.

### Rapamycin decreased $\gamma$ H2AX foci in p21-induced senescence

In HT-p21a cells, senescence caused by p21 was associated with accumulation of H2AX. Rapamycin partially suppressed  $\gamma$ H2AX in these cells (**Fig. 8**). In particular, IPTG arrested these cells in G<sub>1</sub> and G<sub>2</sub> (**Fig. 8**).  $\gamma$ H2AX staining was increased in these cells in both G<sub>1</sub> and G<sub>2</sub>. The amount of  $\gamma$ H2AX in G<sub>2</sub> was higher than the amount of  $\gamma$ H2AX in G<sub>1</sub>, reflecting a double amount of DNA. Rapamycin prevented in part accumulation of  $\gamma$ H2AX

caused by IPTG (**Fig. 8**). In agreement, rapamycin decreased a number of foci per nucleus (**Fig. 9**). Noteworthy, rapamycin partially decreased senescence-associated hypertrophy and senescence caused by IPTG in these cells.<sup>4,5</sup>

## Discussion

Using non-damaging inducers of cellular senescence, we found atypical DNA damage response (DDR) in senescent cells. It is known that cellular senescence is characterized by hyper-activation of nutrient-sensing and pro-inflammatory pathways as a part of over-stressed phenotype. Therefore, atypical DDR may be a marker of cellular hyper-activation. Furthermore, markers of cellular over-activation may vary in senescent cells and perhaps are not obligatory. For example, oncogene-induced senescence is not necessarily accompanied by DDR in rodent primary fibroblasts.<sup>17</sup> We showed that DDR in senescent cells may occur without detectable DNA damage as measured directly by comet assay. Although comet assay is the most sensitive direct method of DNA damage, its sensitivity is limited. Certainly, we cannot exclude DNA damage below a detection limit, but we have no reasons to suggest its presence either, especially given that non-damaging agents were used to cause senescence-associated DDR. In any case, a high magnitude of DDR in senescent cells was dis-proportional to undetectable DNA damage (in comparison with easily detectable comets caused by radiation and DNA damaging drugs).  $\gamma$ H2AX could be also a marker of telomere dysfunction in proliferating cells.<sup>18</sup> Since we studied telomere-independent p21-induced senescence in tumor cells, telomere erosion as a cause of DDR could be excluded.

Histone acetylation may induce local relaxation of chromatin structure. This, in turn, may result in phosphorylation of H2AX.<sup>19</sup> It seems that activation of ATM is not necessary for H2AX phosphorylation caused by NaB as phosphorylation and nuclear translocation of ATM takes place later. We suggest that H2AX histone acetylation caused by HDAC inhibitors promote its phosphorylation even in the absence of DNA breaks. It was shown that phosphorylation of  $\gamma$ H2AX could occur in the absence of DNA damage.<sup>20-23</sup> In such cases, 53BP1 and  $\gamma$ H2AX are not necessarily colocalized.<sup>22</sup> Similarly, H2AX is phosphorylated during mitosis independent from DNA damage.<sup>24,25</sup> Interestingly, so-called DNA damage foci in mitosis are devoid of 53BP1.<sup>26</sup>

Also heat shock activated DDR without DNA breaks<sup>27,28</sup> and the hyperthermia-induced  $\gamma$ H2AX-pATM foci do not contain 53BP1.<sup>27</sup> As another example, phosphorylation of  $\gamma$ H2AX was detected in cells unable to become quiescent.<sup>29</sup> In addition, ATM is not exclusively activated by DNA damage but was shown to be a mediator of insulin signaling, with a crosstalk between Akt and ATM.<sup>30,31</sup> Also, activation of ATM was observed during cell differentiation.<sup>32</sup> This supports our suggestion that phosphorylation of H2AX in senescent cells may not be caused by DNA damage. This may explain DDR under non-DNA damaging conditions<sup>33-35</sup> as well as perfect survival of such pseudo-damaged cells.<sup>34</sup>

Interestingly serum-stimulation causes DDR in fibroblasts undergoing senescence.<sup>36</sup> It was shown that by activating mTOR serum-stimulation leads to senescence when the cell cycle is arrested.<sup>4</sup> Taken together, these two publications suggest that (1) serum-stimulated DDR may be a marker of senescence not a marker of DNA damage and (2) mTOR-dependent

senescence may be manifested by DDR. In fact, we showed here that rapamycin partially prevented H2AX phosphorylation in senescent cells.

To distinguish DDR in senescent cells, we suggest the term pseudo-DDR. First, there is either no DNA damage or very low DNA damage that is non-proportional to the magnitude of pseudo-DDR. Second, pseudo-DDR is not a cause but rather a consequence of senescence. Third, pseudo-DDR includes different events compared with DDR caused by DNA damage. Fourth, pseudo-DDR is in part mTOR dependent. Our data may challenge the dogma that aging is caused by accumulation of DNA damage because detection of some markers of DDR in senescent cells does not prove that aging is caused by DNA damage. Thus, pseudo-DDR may be a marker of cellular activation typical for senescent cells. The concept of senescence-associated mTOR-dependent pseudo-DDR is in agreement with an observation that Wnt-induced senescence was associated with phosphorylation of H2AX preventable by rapamycin.<sup>37</sup> We also suggest a new interpretation of mitogen-induced DDR, which is associated with ROS production and inhibited by 2-deoxy-D-glucose.<sup>38-40</sup> Noteworthy, that ROS activate mTOR pathway, (reviewed in ref. 41) whereas 2-deoxy-D-glucose inhibits mTOR.<sup>42</sup> It is possible that activation of ATM and H2AX during mitogenic stimulation is mTOR-dependent pseudo-DDR.

What is the significance of pseudo-DDR in senescent cells? As recently demonstrated by Campisi and co-workers, DDR stimulates secretion of pro-inflammatory cytokines.<sup>43,44</sup> This in turn reinforces senescence<sup>45,46</sup> and links senescence to diseases of aging, including cancer.<sup>6,9</sup> Senescence-associated secretion depends on DDR but not on DNA damage.<sup>43</sup> And as we demonstrated here, pseudo-DDR can be inhibited by rapamycin.

## Materials and Methods

### Cell lines and reagents

E1A + Ras cells (Eras cells) were established by calcium phosphate transfection of rat and mouse embryonic fibroblasts by E1A Ad5 and activated c-Ha-Ras onco-genes as overgrowth foci on fibroblast monolayers.<sup>13</sup> E1A + Ras cells were maintained in DMEM with 10% FCS and gentamycin. HT-p21 and HT-p21a cells are derivatives of HT1080 human fibrosarcoma cells, where p21 expression can be turned on or off using a physiologically neutral agent isopropyl-b-thio-galactosidase (IPTG).<sup>14,15</sup> HT-p21 cells, also known as clone p21-9, express GFP, whereas HT-p21a cells do not. HT-p16, a derivative of HT1080 human fibrosarcoma cells, where p16 expression can be turned on or off using IPTG.<sup>14,15</sup> Rapamycin was obtained from LC Laboratories and dissolved in DMSO as 2 mM solution and was used at final concentration of 500 nM, unless otherwise indicated. Doxorubicin (DOX), IPTG, sodium butyrate, hydrogen peroxide, topotecan and FC2 were obtained from Sigma-Aldrich (St. Louis, MO). IPTG was dissolved in water as 50 mg/ml stock solution and used in cell culture at final concentration of 50 mg/ml. Cells were exposed to X-rays on ice, after that warm media was added and cells were fixed at the indicated time.

## Immunofluorescence

Cells were seeded on coverslips, washed in 2x PBS (phosphate-buffered solution), fixed in 4% paraformaldehyde for 15 min at room temperature, and permeabilized with 0.5% Triton X-100 for 20 min. Cells were rinsed with cold phosphate-buffered saline and incubated in blocking solution (5% BSA [Sigma]) in PBST (PBS with 0.05% Tween-20 [Sigma]). Primary and secondary antibodies were diluted in blocking solution. Samples were incubated (1 h at room temperature or overnight +4°C) with primary gamma- $\gamma$ H2AX antibody (antibody to  $\gamma$ H2AX Ser-139, Cell Signaling) and mouse anti-ATM phospho-Ser1981 (Calbiochem) diluted 1:200, washed with blocking solution and incubated for 1 h with secondary antibody.

## Primary antibodies

53BP1 rabbit polyclonal Santa-Cruz sc-22760 1:100, phospho-Histone H2A.X (Ser 139) Clone JBW301 mouse monoclonal Millipore N 05-636 1:500, Phospho-Histone H2A.X (Ser 139) rabbit polyclonal Cell Signaling N 2577S 1:100, PhosphoDetect Anti-ATM (pSer 1981) mouse monoclonal (10H11.E12) Calbiochem N DR1002 1:200.

## Secondary antibodies

Invitrogen Molecular Probes: Alexa Fluor 568 goat anti-mouse IgG N A11031 1:1,000, Alexa Fluor 568 F(ab')<sub>2</sub> fragment of goat anti-rabbit IgG N A 21069 1:1,000, Alexa Fluor 488 F(ab')<sub>2</sub> fragment of goat anti-mouse IgG N A 11017 1:1,000, Alexa Fluor 488 F(ab')<sub>2</sub> fragment of goat anti-rabbit IgG N A 11070 1:1,000. For laser scanning confocal microscopy analysis, anti-gamma-H2AX primary antibody was either polyclonal (from rabbit) or monoclonal (from mouse), depending on the origin of the antibodies for p-ATM or 53BP1.

## Intensity of fluorescence

The intensity of fluorescence in the nuclei was estimated by using the software program ImageJ (U.S. National Institutes of Health). The background fluorescence level outside of the nucleus was subtracted from the value of the intensity fluorescence inside the nuclei. Digital images were analyzed with IPLab software for Windows version 3.6.4 from Scanalytics, Inc., Fairfax, VA, USA. Software was used for image segmentation and measurement of background area and the area of interest. Images were edited with Photoshop (Adobe Photoshop 6.0; Mountain View, CA). The green (or red) channel of RGB color images was selected for the evaluation of area of interest. Analyzed cell were selected manually for each staining series. It was measured minimum 60 cells per each sample. Results represented intensity of stained areas (cells) were measured and were calculated as (mean-background)\* area of interest. The average meaning was used as a result. Results are expressed as average mean  $\pm$  Standard Error (calculated as Standard deviation/square root of number of analyzed cells).

## Single cell gel electrophoresis assay (comet assay)

Comet assay was performed as described before. Object-plates were covered by 0.5% agarose, cell suspension 20,000 cells was mixed with 0.6% of low-melting agarose (Sigma)



at 37°C, poured on the object-plate and covered by a cover-slip. After gel formation the cover-slip was removed and agarose layer was covered by another layer of cell-free agarose gel. Cell lysis was carried out in a solution (2.5 M NaCl, 0.1 M EDTA, 10 mM tris-HCl pH 10.0, 1% Triton X-100). Electrophoresis was carried out in alkaline buffer containing 0.3 M NaOH, 1 mM EDTA, pH 13.0 or in neutral TBE buffer. After electrophoresis, the gels were stained by ethidium bromide and visualized with fluorescent microscope Axioscope, Zeiss.<sup>45</sup> In addition, neutral and alkaline comet assays were performed according to the protocol in the CometAssay™ kit (TREVIGEN, Inc., Gaithersburg, MD) with some modifications.<sup>47</sup> For both alkaline and neutral assays all steps were carried out on ice or in the cold to minimize repair processes. For each data point two to three areas on parallel slides were scored with 40–60 cells each. The number and percent of comets was calculated for each area and the presented values are the means of the medians of each data point. At least three independent experiments were performed.

### **γH2AX staining and flow cytometry**

HT-p21a and HT-p16 cells were treated with different concentration of drugs, treated with trypsin, rinsed with PBS, and then fixed in a freshly prepared 2% PFA at 0°C for 15 min, suspension in 1% methanol-free formaldehyde (Polysciences, Warrington, PA) in PBS at 0°C for 15 min, then resuspended in 70% ethanol for at least 2 h at –20°C. The cells were then washed twice in PBS and suspended in 0.2% Triton X-100 (Sigma) in a 1% (w/v) solution of BSA (Sigma) in PBS for 30 min to suppress nonspecific Ab binding. The cells were centrifuged again (200 g, 5 min) and the cell pellet was suspended in 1% BSA in TBFP containing anti-histone γH2AX. The cells were then incubated overnight at 4°C, washed twice with PBS, and resuspended in 1:200 diluted FITC-conjugated F(ab)2 fragment of swine anti-rabbit immunoglobulin (DAKO, Carpinteria, CA) or AlexaFluor-488 conjugated goat anti-rabbit F(ab')2 fragment (Invitrogen, USA) for 30 min in room temperature in the dark. After washing with blocking solution, cells were counterstained with 10 mg/ml propidium iodide (Sigma) dissolved in PBS containing 100 mg/ml RNase A (Sigma) for 30 min at room temperature. Cellular fluorescence was measured using a FACScan flow cytometer (Becton-Dickinson).

### **Supplementary Material**

Refer to Web version on PubMed Central for supplementary material.

### **Acknowledgements**

This work was supported in part by grants of the Russian Foundation for Basic Research (RFBR) (07-04-01537 and 09-04-00466), CGP grant from CRDF-RFBR (RUB1-2868-ST-07/07-04-91154) and grant of the Russian Academy of Sciences (MCB RAS) to T.V.P. and V.A.P. and NIH grant CA 75179 to A.V.G.

### **References**

1. Celeste A, Petersen S, Romanienko PJ, Fernandez-Capetillo O, Chen HT, Sedelnikova OA, et al. Genomic instability in mice lacking histone H2AX. *Science*. 2002; 296:922–7. [PubMed: 11934988]
2. Bassing CH, Alt FW. H2AX May Function as an Anchor to Hold Broken Chromosomal DNA Ends in Close Proximity. *Cell Cycle*. 2008; 3:149–53. [PubMed: 14712078]

3. Fernandez-Capetillo O, Celeste A, Nussenzweig A. Focusing on foci: H2AX and the recruitment of DNA-damage response factors. *Cell Cycle*. 2003; 2:426–7. [PubMed: 12963833]
4. Demidenko ZN, Blagosklonny MV. Growth stimulation leads to cellular senescence when the cell cycle is blocked. *Cell Cycle*. 2008; 7:3355–61. [PubMed: 18948731]
5. Demidenko ZN, Zubova SG, Bukreeva EI, Pospelov VA, Pospelova TV, Blagosklonny MV. Rapamycin decelerates cellular senescence. *Cell Cycle*. 2009; 8:1888–95. [PubMed: 19471117]
6. Campisi J. Senescent cells, tumor suppression and organismal aging: good citizens, bad neighbors. *Cell*. 2005; 120:513–22. [PubMed: 15734683]
7. Campisi J, D'Adda di Fagagna F. Cellular senescence: when bad things happen to good cells. *Nat Rev Mol Cell Biol*. 2007; 8:729–40. [PubMed: 17667954]
8. Blagosklonny MV. Aging-suppressants: cellular senescence (hyperactivation) and its pharmacological deceleration. *Cell Cycle*. 2009; 8:1883–5. [PubMed: 19448395]
9. Patil CK, Mian IS, Campisi J. The thorny path linking cellular senescence to organismal aging. *Mech Ageing Dev*. 2005; 126:1040–5. [PubMed: 16153470]
10. Zhuang D, Mannava S, Grachtchouk V, Tang WH, Patil S, Wawrzyniak JA, et al. C-MYC overexpression is required for continuous suppression of oncogene-induced senescence in melanoma cells. *Oncogene*. 2008; 27:6623–34. [PubMed: 18679422]
11. Demidenko ZN, Shtutman M, Blagosklonny MV. Pharmacologic inhibition of MEK and PI-3K converges on the mTOR/S6 pathway to decelerate cellular senescence. *Cell Cycle*. 2009; 8
12. Abraham RT. PI 3-kinase related kinases: 'big' players in stress-induced signaling pathways. *DNA Repair (Amst)*. 2004; 3:883–7. [PubMed: 15279773]
13. Abramova MV, Pospelova TV, Nikulenkov FP, Hollander CM, Fornace AJJ, Pospelov VA. G<sub>1</sub>/S arrest induced by histone deacetylase inhibitor sodium butyrate in E1A<sub>+</sub> Ras-transformed cells is mediated through downregulation of E2F activity and stabilization of beta-catenin. *J Biol Chem*. 2006; 281:21040–51. [PubMed: 16717102]
14. Chang BD, Broude EV, Fang J, Kalinichenko TV, Abdryashitov R, Poole JC, et al. p21<sup>Waf1/Cip1/Sdi1</sup>-induced growth arrest is associated with depletion of mitosis-control proteins and leads to abnormal mitosis and endoreduplication in recovering cells. *Oncogene*. 2000; 19:2165–70. [PubMed: 10815808]
15. Chang BD, Broude EV, Dokmanovic M, Zhu H, Ruth A, Xuan Y, et al. A senescence-like phenotype distinguishes tumor cells that undergo terminal proliferation arrest after exposure to anticancer agents. *Cancer Res*. 1999; 59:3761–7. [PubMed: 10446993]
16. Korotochkina L, Demidenko ZN, Gudkov AV, Blagosklonny MV. Cellular quiescence caused by the mdm-2 inhibitor nutlin-3A. *Cell Cycle*. 2009; 8:3777–81. [PubMed: 19855165]
17. Efeyan A, Murga M, Martinez-Pastor B, Ortega-Molina A, Soria R, Collado M, et al. Limited role of murine ATM in oncogene-induced senescence and p53-dependent tumor suppression. *PLoS ONE*. 2009; 4:5475.
18. Nakamura AJ, Redon CE, Bonner WM, Sedelnikova OA. Telomere-dependent and telomere-independent origins of endogenous DNA damage in tumor cells. *Aging*. 2009; 1:212–8. [PubMed: 20157510]
19. Ikura T, Tashiro S, Kakino A, Shima H, Jacob N, Amunugama R, et al. DNA damage-dependent acetylation and ubiquitination of H2AX enhances chromatin dynamics. *Mol Cell Biol*. 2007; 27:7028–40. [PubMed: 17709392]
20. Soutoglou E, Misteli T. Activation of the cellular DNA damage response in the absence of DNA lesions. *Science*. 2008; 320:1507–10. [PubMed: 18483401]
21. Soutoglou E. DNA lesions and DNA damage response: even long lasting relationships need a "break". *Cell Cycle*. 2008; 7:3653–8. [PubMed: 19029795]
22. Ziegler-Birling C, Helmrich A, Tora L, Torres-Padilla ME. Distribution of p53 binding protein 1 (53BP1) and phosphorylated H2A.X during mouse preimplantation development in the absence of DNA damage. *Int J Dev Biol*. 2009; 53:1003–11. [PubMed: 19598117]
23. Chuykin IA, Lianguzova MS, Pospelova TV, Pospelov VA. Activation of DNA damage response signaling in mouse embryonic stem cells. *Cell Cycle*. 2008; 7:2922–8. [PubMed: 18787397]



24. Ichijima Y, Sakasai R, Okita N, Asahina K, Mizutani S, Teraoka H. Phosphorylation of histone H2AX at M phase in human cells without DNA damage response. *Biochem Biophys Res Commun.* 2005; 336:807–12. [PubMed: 16153602]
25. McManus KJ, Hendzel MJ. ATM-dependent DNA damage-independent mitotic phosphorylation of H2AX in normally growing mammalian cells. *Mol Biol Cell.* 2005; 16:5013–25. [PubMed: 16030261]
26. Nelson G, Buhmann M, von Zglinicki T. DNA damage foci in mitosis are devoid of 53BP1. *Cell Cycle.* 2009; 8:3379–83. [PubMed: 19806024]
27. Laszlo A, Fleischer I. The heat-induced gamma-H2AX response does not play a role in hyperthermic cell killing. *Int J Hyperthermia.* 2009; 25:199–209. [PubMed: 19437236]
28. Hunt CR, Pandita RK, Laszlo A, Higashikubo R, Agarwal M, Kitamura T, et al. Hyperthermia activates a subset of ataxia-telangiectasia mutated effectors independent of DNA strand breaks and heat shock protein 70 status. *Cancer Res.* 2007; 67:3010–7. [PubMed: 17409407]
29. Perucca P, Cazzalini O, Madine M, Savio M, Laskey RA, Vannini V, et al. Loss of p21 CDKN1A impairs entry to quiescence and activates a DNA damage response in normal fibroblasts induced to quiescence. *Cell Cycle.* 2009; 8:105–14. [PubMed: 19106607]
30. Viniegra JG, Martínez N, Modirassari P, Losa JH, Parada Cobo C, Lobo VJ, et al. Full activation of PKB/Akt in response to insulin or ionizing radiation is mediated through ATM. *J Biol Chem.* 2005; 280:4029–36. [PubMed: 15546863]
31. Suzuki A, Kusakai G, Kishimoto A, Lu J, Ogura T, Lavin MF, et al. Identification of a novel protein kinase mediating Akt survival signaling to the ATM protein. *J Biol Chem.* 2003; 278:48–53. [PubMed: 12409306]
32. Fernandes ND, Sun Y, Price BD. Activation of the kinase activity of ATM by retinoic acid is required for CREB-dependent differentiation of neuroblastoma cells. *J Biol Chem.* 2007; 282:16577–84. [PubMed: 17426037]
33. Sokolov MV, Dickey JS, Bonner WM, Sedelnikova OA. gamma-H2AX in bystander cells: not just a radiation-triggered event, a cellular response to stress mediated by intercellular communication. *Cell Cycle.* 2003; 2:426–7. [PubMed: 12963833]
34. Dmitrieva NI, Burg MB. Living with DNA breaks is an everyday reality for cells adapted to high NaCl. *Cell Cycle.* 2004; 3:561–3. [PubMed: 15107607]
35. Blazkova H, Krejcikova K, Moudry P, Frisan T, Hodny Z, Bartek J. Bacterial Intoxication Evokes Cellular Senescence with Persistent DNA Damage and Cytokine Signaling. *J Cell Mol Med.* 2009
36. Satyanarayana A, Greenberg RA, Schaetzlein S, Buer J, Masutomi K, Hahn WC, et al. Mitogen stimulation cooperates with telomere shortening to activate DNA damage responses and senescence signaling. *Mol Cell Biol.* 2004; 24:5459–74. [PubMed: 15169907]
37. Castilho RM, Squarize CH, Chodosh LA, Williams BO, Gutkind JS. mTOR mediates Wnt-induced epidermal stem cell exhaustion and aging. *Cell Stem Cell.* 2009; 5:279–89. [PubMed: 19733540]
38. Tanaka T, Halicka HD, Traganos F, Darzynkiewicz Z. Phosphorylation of histone H2AX on Ser 139 and activation of ATM during oxidative burst in phorbol ester-treated human leukocytes. *Cell Cycle.* 2006; 5:2671–5. [PubMed: 17106266]
39. Tanaka T, Kurose A, Halicka HD, Traganos F, Darzynkiewicz Z. 2-deoxy-D-glucose reduces the level of constitutive activation of ATM and phosphorylation of histone H2AX. *Cell Cycle.* 2006; 5:878–82. [PubMed: 16628006]
40. Tanaka T, Kajstura M, Halicka HD, Traganos F, Darzynkiewicz Z. Constitutive histone H2AX phosphorylation and ATM activation are strongly amplified during mitogenic stimulation of lymphocytes. *Cell Prolif.* 2007; 40:1–13. [PubMed: 17227291]
41. Blagosklonny MV. Aging: ROS or TOR. *Cell Cycle.* 2008; 7:3344–54. [PubMed: 18971624]
42. Jiang W, Zhu Z, HJ T. Modulation of the activities of AMP-activated protein kinase, protein kinase B, and mammalian target of rapamycin by limiting energy availability with 2-deoxyglucose. *Mol Carcinog.* 2008; 47:616–28. [PubMed: 18247380]
43. Rodier F, Coppé JP, Patil CK, Hoeijmakers WA, Muñoz DP, Raza SR, et al. Persistent DNA damage signalling triggers senescence-associated inflammatory cytokine secretion. *Nat Cell Biol.* 2009; 11:973–9. [PubMed: 19597488]

44. Bhaumik D, Scott GK, Schokrpur S, Patil CK, Orjalo AV, Rodier F, et al. MicroRNAs miR-146a/b negatively modulate the senescence-associated inflammatory mediators IL-6 and IL-8. *Aging*. 2009; 1:402–11. [PubMed: 20148189]
45. Acosta JC, O'Loughlen A, Banito A, Raguz S, Gil J. Control of senescence by CXCR2 and its ligands. *Cell Cycle*. 2008; 7:2956–9. [PubMed: 18838863]
46. Kuilman T, Michaloglou C, Vredeveld LC, Douma S, van Doorn R, Desmet CJ, et al. Oncogene-induced senescence relayed by an interleukin-dependent inflammatory network. *Cell*. 2008; 133:1019–31. [PubMed: 18555778]
47. Tanaka T, Kurose A, Halicka HD, Huang X, Traganos F, Darzynkiewicz Z. Nitrogen oxide-releasing aspirin induces histone H2AX phosphorylation, ATM activation and apoptosis preferentially in S-phase cells: involvement of reactive oxygen species. *Cell Cycle*. 2006; 5:1669–74. [PubMed: 16861926]

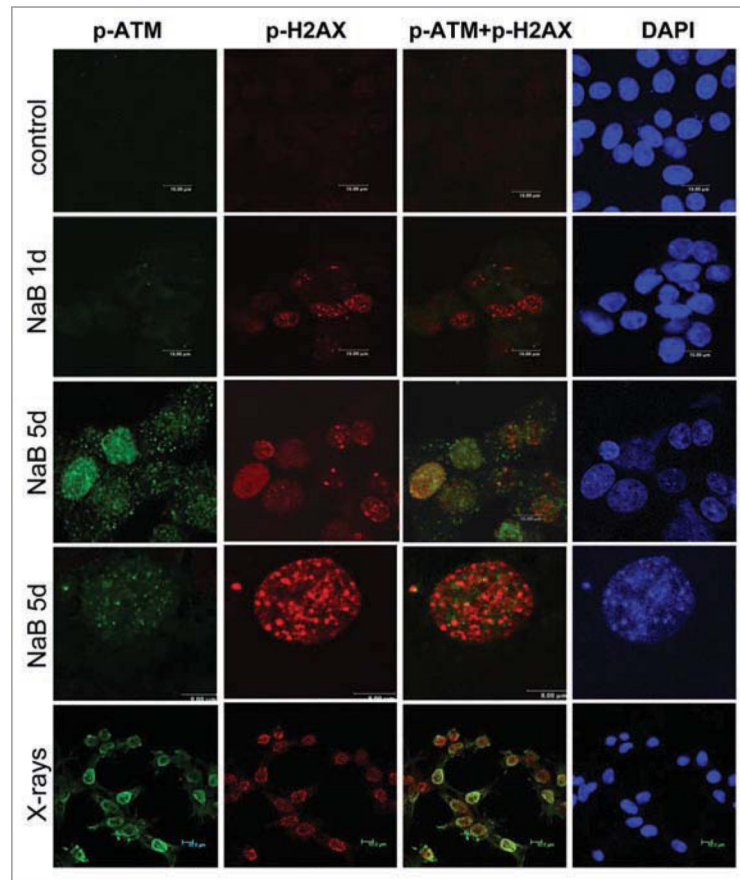


**Figure 1.** Immunofluorescence for  $\gamma$ H2AX and p-ATM in NaB-treated E1A + Ras cells. Representative images of E1A + Ras cells stained for  $\gamma$ H2AX (Ser139) and p-ATM (Ser 1981) at various time points. Cells were treated with NaB and then fixed at 24, 72, 120 hr. Immunofluorescence of  $\gamma$ H2AX (red) and p-ATM (green), nuclei were stained with DAPI (blue), scale 10  $\mu$ m. Bottom panel: Higher magnification (scale 5  $\mu$ m).  $\gamma$ H2AX foci accumulation at 5 days of NaB treatment.

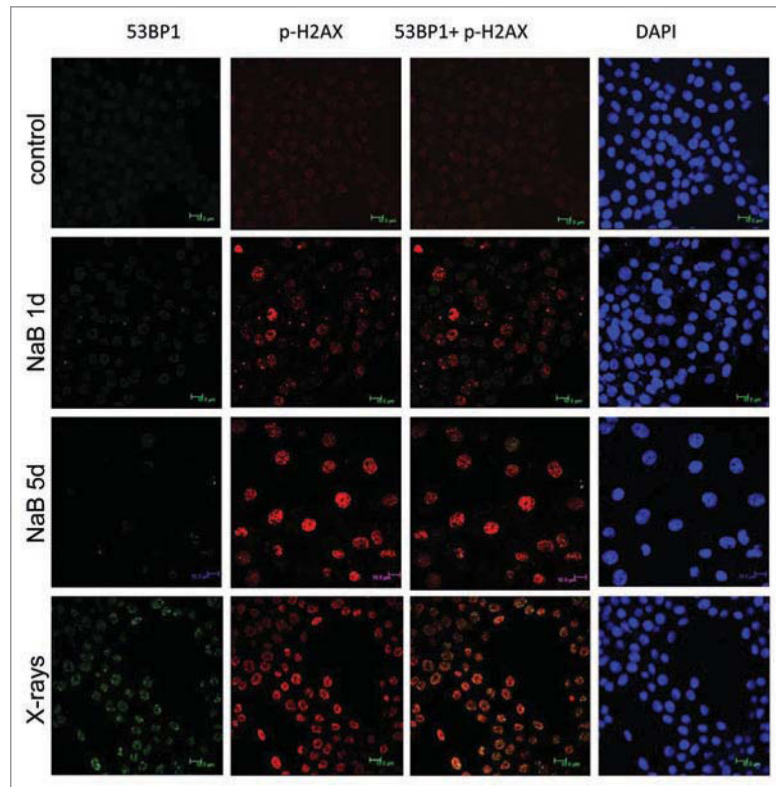


**Figure 2.** 53BP1 and  $\gamma$ H2AX foci in NaB-treated and irradiated E1A + Ras cells. Representative images of E1A + Ha-ras cells stained for  $\gamma$ H2AX (Ser139) and 53BP1 following NaB treatment (5 d) or irradiation (positive control). Immunofluorescence of  $\gamma$ H2AX (red) and 53BP1 (green), nuclei were stained with DAPI (blue), scale 10  $\mu$ m. Bottom panel: Irradiation.

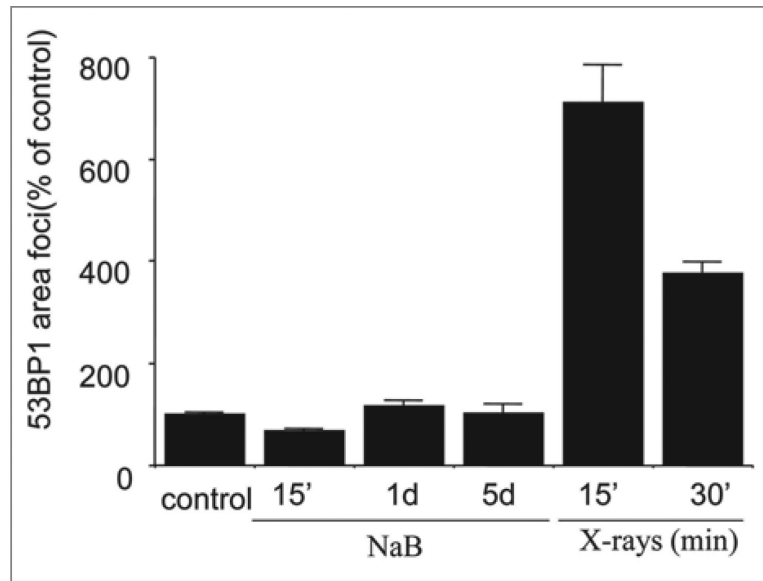


**Figure 3.**

53BP1 foci area in NaB treated and irradiated E1A + Ras cells. Cells were treated with NaB 15 min (15'), 1 day and 5 days or irradiated (6 Gy) and incubated for 15 min or 30 min before fixation. IPLab software was used for quantification of the focus area. Approximately 100 cells were analyzed for each time point. Bars indicate Standard Error (SE). Results are shown as percent of control (no treatment).

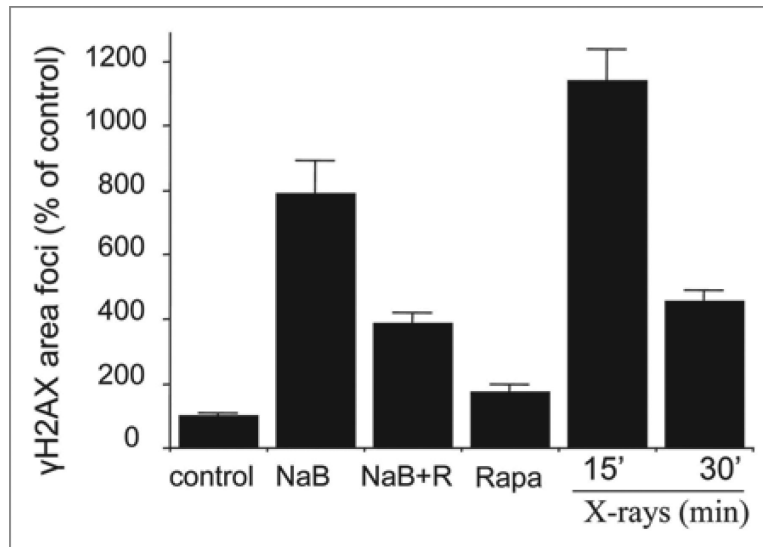


**Figure 4.**

Effect of rapamycin on  $\gamma$ H2AX foci accumulation in NaB treated E1A + Ras cells. Cells were treated with NaB for 5 days or irradiated (1 Gy) for 15 min and 30 min (X-rays: 15 and 30) before fixation (positive control). IPLab software was used for quantification of the focus area. Approximately 100 cells were analyzed for each time point. Bars indicate Standard Error (SE). Results are shown as percent of control (no treatment).



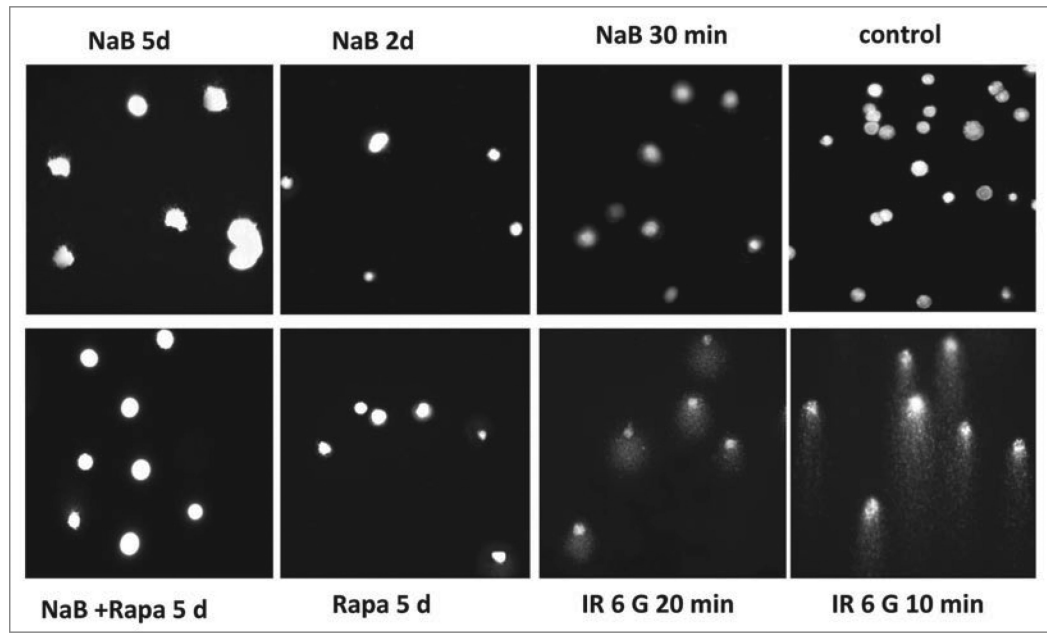


**Figure 5.**

Analysis of DNA breaks in E1A + Ras cells. E1A + Ras cells were subjected to single-cell gel electrophoresis under denaturing conditions (comet assay). Cells were gamma-irradiated for 10 min and 20 min or treated with NaB, Rapamycin (Rapa) or a combination of NaB and Rapa at indicated time points. Images of ethidium bromide-stained DNA comets and nuclei were obtained at magnification x200.

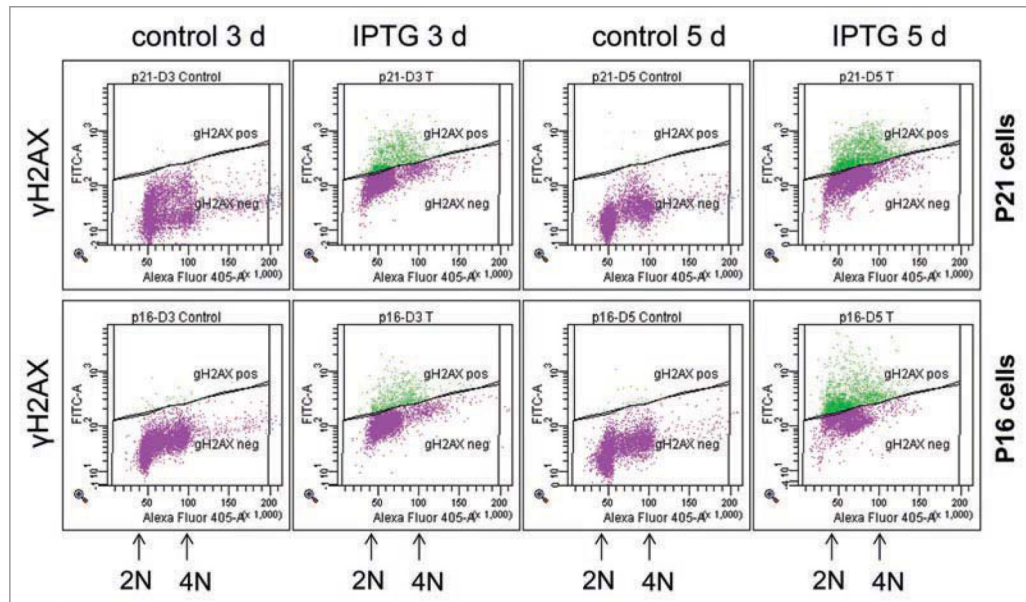


**Figure 6.**

p21- and p16-induced  $\gamma$ H2AX phosphorylation in senescent HT-p21a and HT-p16 cells. HT-p21a cells (upper) and HT-p16 cells (low) were treated with IPTG for 3 days and 5 days or left untreated (control). Results are present as DNA content (X-axis) vs.  $\gamma$ H2AX levels (Y-axis).

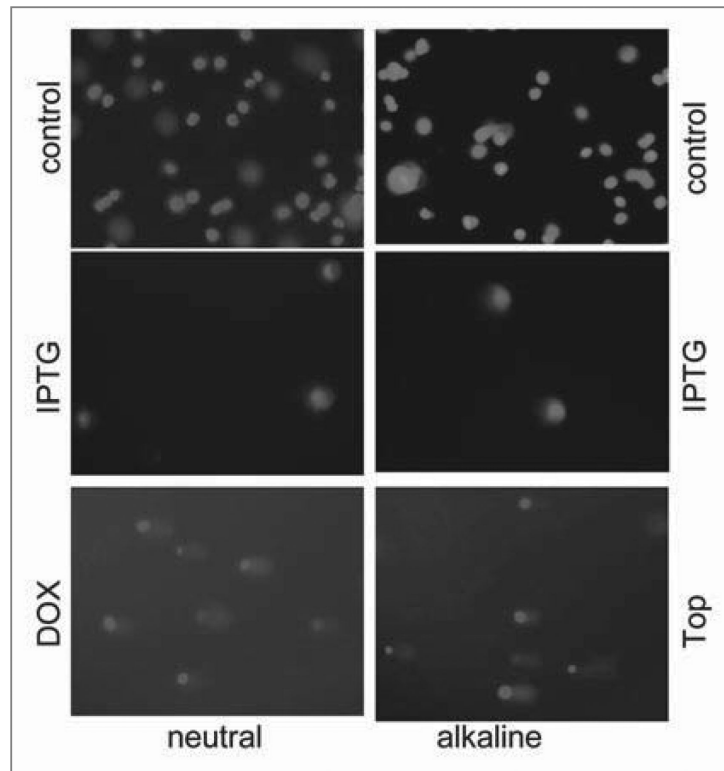


**Figure 7.**

Analysis of DNA breaks in senescent HT-p21a cells by comet assay. HT-p21a cells were treated with IPTG for 4 days or left untreated (control). As a positive control cells were treated with DNA-damaging drugs (DDD): doxorubicin (Dox), which causes double strand breaks, or topotecan (Top), which causes mostly single strand breaks. Then cells were subjected to single-cell gel DNA electrophoresis (at neutral and alkaline conditions). Bottom panel: deleted

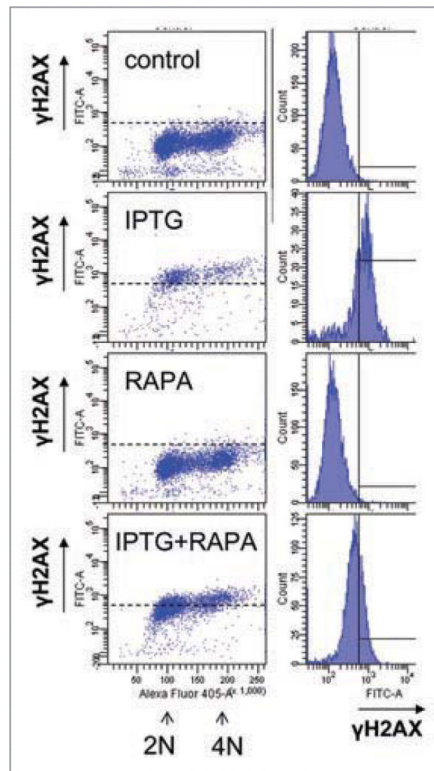


**Figure 8.**

Effect of rapamycin on  $\gamma$ H2AX phosphorylation in senescent cells. HT-p21a cells (deleted) and HT-p16 cells (low) were treated with IPTG, rapamycin (RAPA) or IPTG + Rapa for 4 days. (A) Left column: DNA content (X-axis) vs. H2AX levels (Y-axis). (B) Right column:  $\gamma$ H2AX levels (X-axis) vs. cell count (Y-axis).

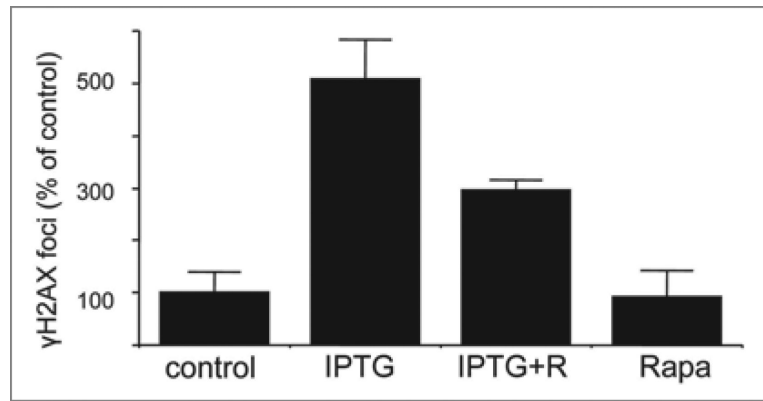


**Figure 9.** Effects of rapamycin on accumulation of  $\gamma$ H2AX foci in HT-p21a senescent cells. HT-p21a cells were treated with IPTG, rapamycin (RAPA) or IPTG + Rapa for 3 days. Slides were fixed and stained for  $\gamma$ H2AX. Foci per nucleus were counted. Results are shown as percent of control (no treatment).